

## Critical Scaling of Shear Viscosity at the Jamming Transition

Peter Olsson<sup>1</sup> and S. Teitel<sup>2</sup>

<sup>1</sup>*Department of Physics, Umeå University, 901 87 Umeå, Sweden*

<sup>2</sup>*Department of Physics and Astronomy, University of Rochester, Rochester, New York 14627, USA*

(Received 13 April 2007; published 26 October 2007)

We carry out numerical simulations to study transport behavior about the jamming transition of a model granular material in two dimensions at zero temperature. Shear viscosity  $\eta$  is computed as a function of particle volume density  $\rho$  and applied shear stress  $\sigma$ , for diffusively moving particles with a soft core interaction. We find an excellent scaling collapse of our data as a function of the scaling variable  $\sigma/|\rho_c - \rho|^\Delta$ , where  $\rho_c$  is the critical density at  $\sigma = 0$  (“point  $J$ ”), and  $\Delta$  is the crossover scaling critical exponent. We define a correlation length  $\xi$  from velocity correlations in the driven steady state and show that it diverges at point  $J$ . Our results support the assertion that jamming is a true second-order critical phenomenon.

DOI: 10.1103/PhysRevLett.99.178001

PACS numbers: 45.70.-n, 64.60.-i

In granular materials, or other spatially disordered systems such as colloidal glasses, gels, and foams, in which thermal fluctuations are believed to be negligible, a *jamming transition* has been proposed: upon increasing the volume density (or “packing fraction”) of particles  $\rho$  above a critical  $\rho_c$ , the sudden appearance of a finite shear stiffness signals a transition between flowing liquid and rigid (but disordered) solid states [1]. It has further been proposed by Liu and Nagel and co-workers [2,3] that this jamming transition is a special second-order critical point (“point  $J$ ”) in a wider phase diagram whose axes are volume density  $\rho$ , temperature  $T$ , and applied shear stress  $\sigma$  (the latter parameter taking one out of equilibrium to nonequilibrium driven steady states). A surface in this three-dimensional parameter space then separates jammed from flowing states, and the intersection of this surface with the equilibrium  $\rho$ - $T$  plane at  $\sigma = 0$  is related to the structural glass transition.

Several numerical [3–10], theoretical [11–14], and experimental [5,15–18] works have investigated the jamming transition, mostly by considering behavior as the transition is approached from the *jammed* side. In this work we consider the *flowing* state, computing the shear viscosity  $\eta$  under applied uniform shear stress. Previous works have simulated the flowing response to applied shear in glassy systems at finite temperature [19–21], and in foams [4] and granular systems [10] at  $T = 0$ ,  $\rho > \rho_c$ . Here we consider the  $\rho$ - $\sigma$  plane at  $T = 0$ , showing for the first time that, near point  $J$ ,  $\eta^{-1}(\rho, \sigma)$  collapses to a universal scaling function of the variable  $\sigma/|\rho_c - \rho|^\Delta$  for both  $\rho < \rho_c$  and  $\rho > \rho_c$ . We further define a correlation length  $\xi$  from steady state velocity correlations and show that it diverges at point  $J$ . Our results support that jamming is a true second-order critical phenomenon.

Following O’Hern *et al.* [3], we simulate frictionless soft disks in two dimensions (2D) using a bidisperse mixture with equal numbers of disks of two different radii. The radii ratio is 1.4 and the interaction between the particles is

$$V(r_{ij}) = \begin{cases} \epsilon(1 - r_{ij}/d_{ij})^2/2 & \text{for } r_{ij} < d_{ij} \\ 0 & \text{for } r_{ij} \geq d_{ij} \end{cases}, \quad (1)$$

where  $r_{ij}$  is the distance between the centers of two particles  $i$  and  $j$ , and  $d_{ij}$  is the sum of their radii. Particles are noninteracting when they do not touch, and they interact with a harmonic repulsion when they overlap. We measure length in units such that the smaller diameter is unity, and we measure energy in units such that  $\epsilon = 1$ . A system of  $N$  disks in an area  $L_x \times L_y$  thus has a volume density

$$\rho = N\pi(0.5^2 + 0.7^2)/(2L_x L_y). \quad (2)$$

To model an applied uniform shear stress,  $\sigma$ , we first use Lees-Edwards boundary conditions [22] to introduce a uniform shear *strain*,  $\gamma$ . Defining particle  $i$ ’s position as  $\mathbf{r}_i = (x_i + \gamma y_i, y_i)$ , we apply periodic boundary conditions on the coordinates  $x_i$  and  $y_i$  in an  $L_x \times L_y$  system. In this way, each particle upon mapping back to itself under the periodic boundary condition in the  $\hat{y}$  direction has displaced a distance  $\Delta x = \gamma L_y$  in the  $\hat{x}$  direction, resulting in a shear strain  $\Delta x/L_y = \gamma$ . When particles do not touch, and hence all mutual forces vanish,  $x_i$  and  $y_i$  are constant and a time dependent strain  $\gamma(t)$  produces a uniform shear flow,  $d\mathbf{r}_i/dt = y_i(d\gamma/dt)\hat{x}$ . When particles touch, we assume a diffusive response to the interparticle forces, as would be appropriate if the particles were immersed in a highly viscous liquid or resting upon a rough surface with high friction. This results in the following equation of motion, which was first proposed as a model for sheared foams [4],

$$\frac{d\mathbf{r}_i}{dt} = -D \sum_j \frac{dV(r_{ij})}{d\mathbf{r}_i} + y_i \frac{d\gamma}{dt} \hat{x}. \quad (3)$$

The strain  $\gamma$  is then treated as a dynamical variable, obeying the equation of motion,

$$\frac{d\gamma}{dt} = D_\gamma \left[ L_x L_y \sigma - \sum_{i \neq j} \frac{dV(r_{ij})}{d\gamma} \right], \quad (4)$$

where the applied stress  $\sigma$  acts like an external force on  $\gamma$  and the interaction terms  $V(r_{ij})$  depend on  $\gamma$  via the particle separations,  $\mathbf{r}_{ij} = ([x_i - x_j]_{L_x} + \gamma[y_i - y_j]_{L_y}, [y_i - y_j]_{L_y})$ , where by  $[\dots]_{L_\mu}$  we mean that the difference is to be taken, invoking periodic boundary conditions, so that the result lies in the interval  $(-L_\mu/2, L_\mu/2]$ . The constants  $D$  and  $D_\gamma$  are set by the dissipation of the medium in which the particles are embedded; we take units of time such that  $D = D_\gamma \equiv 1$ .

In a flowing state at finite  $\sigma > 0$ , the sum of the interaction terms is of order  $O(N)$  so that the right-hand side of Eq. (4) is  $O(1)$ . The strain  $\gamma(t)$  increases linearly in time on average, leading to a sheared flow of the particles with average velocity gradient  $dv_x/dy = \langle d\gamma/dt \rangle$ , where  $v_x(y)$  is the average velocity in the  $\hat{x}$  direction of the particles at height  $y$ . We then measure the shear viscosity, defined by

$$\eta \equiv \frac{\sigma}{dv_x/dy} = \frac{\sigma}{\langle d\gamma/dt \rangle}. \quad (5)$$

We expect  $\eta^{-1}$  to vanish in a jammed state.

We integrate the equations of motion, Eqs. (3) and (4), starting from an initial random configuration, using the Heuns method. The time step  $\Delta t$  is varied according to system size to ensure our results are independent of  $\Delta t$ . We consider a fixed number of particles  $N$ , in a square system  $L \equiv L_x = L_y$ , and vary the volume density  $\rho$  by adjusting the length  $L$  according to Eq. (2). We simulate for times  $t_{\text{tot}}$  such that the total relative displacement per unit length transverse to the direction of motion is typically  $\gamma(t_{\text{tot}}) \sim 10$ , with  $\gamma(t_{\text{tot}})$  ranging between 1 and 200 depending on the particular system parameters.

In Fig. 1 we show our results for  $\eta^{-1}$  using a fixed small shear stress,  $\sigma = 10^{-5}$ , representative of the  $\sigma \rightarrow 0$  limit. Our raw results are shown in Fig. 1(a) for several different numbers of particles  $N$  from 64 to 1024. Comparing the curves for different  $N$  as  $\rho$  increases, we see that they overlap for some range of  $\rho$ , before each drops discontinuously into a jammed state. As  $N$  increases, the onset value of  $\rho$  for jamming increases to a limiting value  $\rho_c \simeq 0.84$  (consistent with the value for random close packing [3]) and  $\eta^{-1}$  vanishes continuously. For finite  $N$ , systems jam below  $\rho_c$  because there is always a finite probability to find a configuration with a force chain spanning the width of the system, thus causing it to jam, and at  $T = 0$ , once a system jams, it remains jammed for all further time. As the system evolves dynamically with increasing simulation time, it explores an increasing region of configuration space, and ultimately finds a configuration that causes it to jam. The statistical weight of such jamming configurations decreases, and hence the average time required to jam increases, as one either decreases  $\rho$ , or increases  $N$  [3]. In the limit  $N \rightarrow \infty$ , we expect jamming will occur in finite time

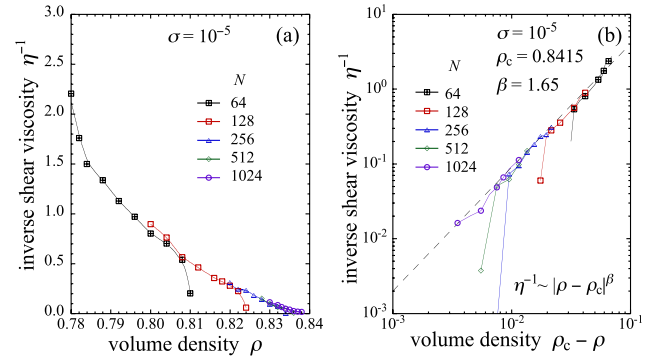


FIG. 1 (color online). (a) Plot of inverse shear viscosity  $\eta^{-1}$  vs volume density  $\rho$  for several different numbers of particles  $N$ , at constant small applied shear stress  $\sigma = 10^{-5}$ . As  $N$  increases, one sees jamming at a limiting value of the density  $\rho_c \sim 0.84$ . (b) Log-log replot of the data of (a) as  $\eta^{-1}$  vs  $\rho_c - \rho$ , with  $\rho_c = 0.8415$ . The dashed line has slope  $\beta = 1.65$  indicating the continuous algebraic vanishing of  $\eta^{-1}$  at  $\rho_c$  with a critical exponent  $\beta$ .

only for  $\rho \geq \rho_c$ . In Fig. 1(b) we show a log-log plot of  $\eta^{-1}$  versus  $\rho_c - \rho$ , using a value  $\rho_c = 0.8415$ . We see that the data in the unjammed state is well approximated by a straight line of slope  $\beta = 1.65$ , giving  $\eta^{-1} \sim |\rho - \rho_c|^\beta$  in agreement with the expectation that point  $J$  is a second-order phase transition.

If point  $J$  is indeed a true critical point, one expects that its influence will be felt also at finite values of the stress  $\sigma$ , with  $\eta^{-1}$  obeying a typical scaling law,

$$\eta^{-1}(\rho, \sigma) = |\rho - \rho_c|^\beta f_\pm \left( \frac{\sigma}{|\rho - \rho_c|^\Delta} \right). \quad (6)$$

Here  $z \equiv \sigma/|\rho - \rho_c|^\Delta$  is the crossover scaling variable,  $\Delta$  is the crossover scaling critical exponent, and  $f_-(z), f_+(z)$  are the two branches of the crossover scaling function for  $\rho < \rho_c$  and  $\rho > \rho_c$ , respectively.

In Fig. 2 we show a log-log plot of inverse shear viscosity  $\eta^{-1}$  versus applied shear stress  $\sigma$ , for several different values of volume density  $\rho$ . Our results are for systems large enough that we believe finite size effects are negligible. We use  $N = 1024$  for  $\rho < 0.844$  and  $N = 2048$  for  $\rho \geq 0.844$ . Again we see that  $\rho_c \simeq 0.8415$  separates two limits of behavior. For  $\rho < \rho_c$ ,  $\log \eta^{-1}$  is convex in  $\log \sigma$ , decreasing to a finite value as  $\sigma \rightarrow 0$ . For  $\rho > \rho_c$ ,  $\log \eta^{-1}$  is concave in  $\log \sigma$ , decreasing towards zero as  $\sigma \rightarrow 0$ . The dashed straight line, separating the two regions of behavior, indicates the power law dependence that is expected exactly at  $\rho = \rho_c$  (see below). Similar power law behavior at  $\rho_c$  was recently found in simulations of a three-dimensional granular material [23].

In Fig. 3 we replot the data of Fig. 2 in the scaled variables  $\eta^{-1}/|\rho - \rho_c|^\beta$  versus  $\sigma/|\rho - \rho_c|^\Delta$ . Using  $\rho_c = 0.8415$ ,  $\beta = 1.65$  [the same values used in Fig. 1(b)] and  $\Delta = 1.2$ , we find an excellent scaling collapse in agreement with the prediction of Eq. (6). As the scaling variable

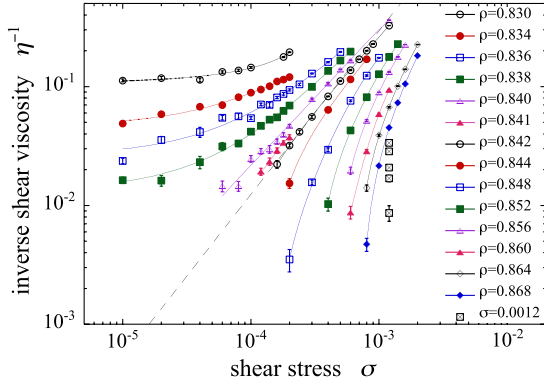


FIG. 2 (color online). Plot of inverse shear viscosity  $\eta^{-1}$  vs applied shear stress  $\sigma$  for several different values of the volume density  $\rho$ . The dashed line represents the power law dependence expected exactly at  $\rho = \rho_c$  and has a slope  $\beta/\Delta = 1.375$ . Solid lines are guides to the eye. Points labeled  $\sigma = 0.0012$  correspond to densities  $\rho = 0.870, 0.872, 0.874, 0.876, \text{ and } 0.878$ .

$z \rightarrow 0$ ,  $f_-(z) \rightarrow \text{const}$ ; this gives the vanishing of  $\eta^{-1} \sim |\rho - \rho_c|^\beta$  at  $\sigma = 0$ . As  $z \rightarrow \infty$ , both branches of the scaling function approach a common curve,  $f_\pm(z) \sim z^{\beta/\Delta}$ , so that precisely at  $\rho = \rho_c$ ,  $\eta^{-1} \sim \sigma^{\beta/\Delta}$  as  $\sigma \rightarrow 0$  [24]. This is shown as the dashed line in both Figs. 2 and 3. A similar scaling collapse of  $\eta$  has been found in simulations [20] of a sheared Lennard-Jones glass, as a function of temperature and applied shear strain rate  $\dot{\gamma}$ , but only above the glass transition,  $T > T_c$ . By comparing the goodness of the scaling collapse as parameters are varied, we estimate the accuracy of the critical exponents to be roughly  $\beta = 1.7 \pm 0.2$  and  $\Delta = 1.2 \pm 0.2$ .

That the crossover scaling exponent  $\Delta > 0$ , implies that  $\sigma$  is a relevant variable in the renormalization group sense

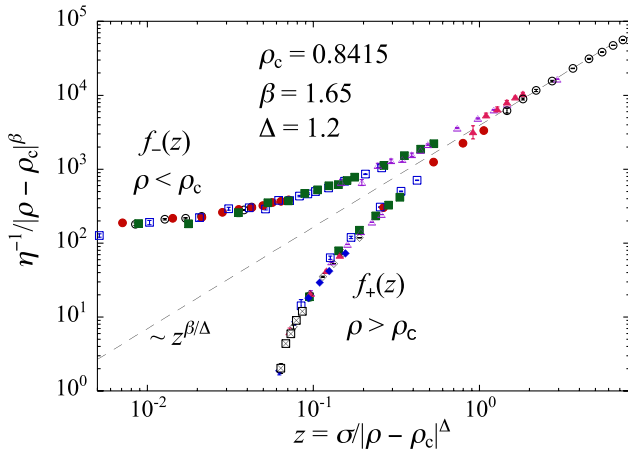


FIG. 3 (color online). Plot of scaled inverse viscosity  $\eta^{-1}/|\rho - \rho_c|^\beta$  vs scaled shear stress  $z \equiv \sigma/|\rho - \rho_c|^\Delta$  for the data of Fig. 2. We find an excellent collapse to the scaling form of Eq. (6) using values  $\rho_c = 0.8415$ ,  $\beta = 1.65$ , and  $\Delta = 1.2$ . The dashed line represents the large  $z$  asymptotic dependence,  $\sim z^{\beta/\Delta}$ . Data point symbols correspond to those used in Fig. 2.

and that critical behavior at finite  $\sigma$  should be in a different universality class from the jamming transition at point  $J$  (i.e.,  $\sigma = 0$ ). The nature of jamming at finite  $\sigma > 0$  will be determined by the behavior of the branch of the crossover scaling function  $f_+(z)$  that describes behavior for  $\rho > \rho_c$ . From Fig. 3 we see that  $f_+(z)$  is a decreasing function of  $z$ . If  $f_+(z)$  vanishes only when  $z \rightarrow 0$ , then Eq. (6) implies that  $\eta^{-1}$  vanishes for  $\rho > \rho_c$  only when  $\sigma = 0$ , and so there will be no jamming at finite  $\sigma > 0$ . If, however,  $f_+(z)$  vanishes at some finite  $z_0$ , then  $\eta^{-1}$  will vanish whenever  $\sigma/(\rho - \rho_c)^\Delta = z_0$ ; there will then be a line of jamming transitions emanating from point  $J$  in the  $\rho - \sigma$  plane given by the curve  $\rho^*(\sigma) = \rho_c + (\sigma/z_0)^{1/\Delta}$ . If  $f_+(z)$  vanishes continuously at  $z_0$ , jamming at finite  $\sigma$  will be like a second-order transition; if  $f_+(z)$  jumps discontinuously to zero at  $z_0$ , it will be like a first-order transition. Such a first-order-like transition has been reported in simulations [20,21] of sheared glasses at finite temperature below the glass transition,  $T < T_c$ . However, recent simulations [10] of a granular system at  $T = 0$ ,  $\rho > \rho_c$ , showed that a similar first-order-like behavior was a finite size effect that vanished in the thermodynamic limit. With these observations, we leave the question of criticality at finite  $\sigma$  to future work.

The critical scaling found in Fig. 3 strongly suggests that point  $J$  is indeed a true second-order phase transition and thus implies that there ought to be a diverging correlation length  $\xi$  at this point. Measurements of dynamic (time dependent) susceptibilities have been used to argue for a divergent length scale in both the thermally driven glass transition [25] and the density driven jamming transition [17]. Here we consider the *equal time* transverse velocity correlation function in the shear driven steady state,

$$g(x) = \langle v_y(x_i, y_i) v_y(x_i + x, y_i) \rangle, \quad (7)$$

where  $v_y(x_i, y_i)$  is the instantaneous velocity in the  $\hat{y}$  direction, transverse to the direction of the average shear flow, for a particle at position  $(x_i, y_i)$ . The average is over particle positions and time. In the inset to Fig. 4 we plot  $g(x)/g(0)$  versus  $x$  for three different values of  $\rho$  at fixed  $\sigma = 10^{-4}$  and number of particles  $N = 1024$ . We see that  $g(x)$  decreases to *negative* values at a well-defined minimum, before decaying to zero as  $x$  increases. We define  $\xi$  to be the position of this minimum. That  $g(\xi) < 0$  indicates that regions separated by a distance  $\xi$  are *anticorrelated*. We can thus interpret the sheared flow in the unjammed state as due to the rotation of correlated regions of length  $\xi$ . Similar behavior, leading to a similar definition of  $\xi$ , has previously been found [26] in correlations of the nonaffine displacements of particles in a Lennard-Jones glass, in response to small elastic distortions.

As with viscosity, we expect the correlation length  $\xi(\rho, \sigma)$  to obey a scaling equation similar to Eq. (6). We consider here the inverse correlation length  $\xi^{-1}$ , which like  $\eta^{-1}$  should vanish at the jamming transition, obeying the

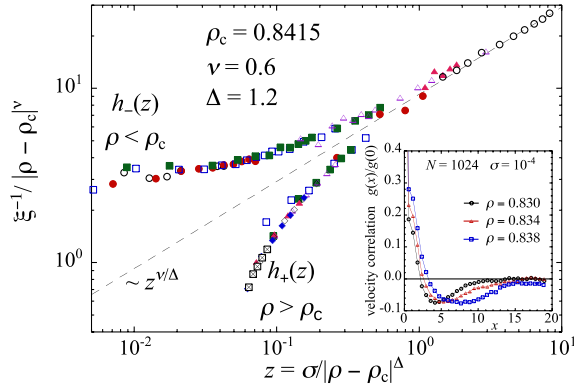


FIG. 4 (color online). Inset: normalized transverse velocity correlation function  $g(x)/g(0)$  vs longitudinal position  $x$  for  $N = 1024$  particles, applied shear stress  $\sigma = 10^{-4}$ , and volume densities  $\rho = 0.830, 0.834$ , and  $0.838$ . The position of the minimum determines the correlation length  $\xi$ . Main figure: plot of scaled inverse correlation length  $\xi^{-1}/|\rho - \rho_c|^\nu$  vs scaled shear stress  $z \equiv \sigma/|\rho - \rho_c|^\Delta$  for the data of Fig. 2. We find a good scaling collapse using values  $\rho_c = 0.8415$ ,  $\Delta = 1.2$  (the same as in Fig. 3), and  $\nu = 0.6$ . Data point symbols correspond to those used in Fig. 2.

scaling equation,

$$\xi^{-1}(\rho, \sigma) = |\rho - \rho_c|^\nu h_\pm\left(\frac{\sigma}{|\rho - \rho_c|^\Delta}\right). \quad (8)$$

The correlation length critical exponent is  $\nu$ , but the cross-over exponent  $\Delta$  remains the same as for the viscosity.

In Fig. 4 we plot the scaled inverse correlation length,  $\xi^{-1}/|\rho - \rho_c|^\nu$ , versus the scaled stress,  $\sigma/|\rho - \rho_c|^\Delta$ . Using  $\rho_c = 0.8415$  and  $\Delta = 1.2$ , as was found for the scaling of  $\eta^{-1}$ , we now find a good scaling collapse for  $\xi^{-1}$  by taking the value  $\nu = 0.6$ . By comparing the goodness of the collapse as  $\nu$  is varied, we estimate  $\nu = 0.6 \pm 0.1$ . From the scaling equation Eq. (8) we expect both branches of the scaling function to approach the power law  $h_\pm(z) \sim z^{\nu/\Delta}$  as  $z \rightarrow \infty$ , so that  $\xi^{-1} \sim \sigma^{\nu/\Delta}$  as  $\sigma \rightarrow 0$  at  $\rho = \rho_c$  [24]. This is shown as the dashed line in Fig. 4. Our result is consistent with the conclusion “ $\nu$  is between 0.6 and 0.7” of Drocco *et al.* [7] for the flowing phase,  $\rho < \rho_c$ . It also agrees with  $\nu = 0.71 \pm 0.08$  found by O’Hern *et al.* [3] from a finite size scaling argument. Wyart *et al.* [14] have proposed a diverging length scale with exponent  $\nu = 0.5$  by considering the vibrational spectrum of soft modes approaching point  $J$  from the jammed side,  $\rho > \rho_c$ . While our results cannot rule out  $\nu = 0.5$ , our scaling collapse in Fig. 4 does seem somewhat better when using the larger value 0.6.

This work was supported by Department of Energy Grant No. DE-FG02-06ER46298 and by the resources of

the Swedish High Performance Computing Center North (HPC2N). We thank J.P. Sethna, L. Berthier, M. Wyart, J.M. Schwarz, N. Xu, D.J. Durian, A.J. Liu, and S.R. Nagel for helpful discussion.

- [1] *Jamming and Rheology*, edited by A.J. Liu and S.R. Nagel (Taylor & Francis, New York, 2001).
- [2] A. J. Liu and S. R. Nagel, *Nature (London)* **396**, 21 (1998).
- [3] C. S. O’Hern *et al.*, *Phys. Rev. E* **68**, 011306 (2003).
- [4] D. J. Durian, *Phys. Rev. Lett.* **75**, 4780 (1995); *Phys. Rev. E* **55**, 1739 (1997).
- [5] H. A. Makse, D. L. Johnson, and L. M. Schwartz, *Phys. Rev. Lett.* **84**, 4160 (2000).
- [6] C. S. O’Hern *et al.*, *Phys. Rev. Lett.* **86**, 111 (2001); **88**, 075507 (2002).
- [7] J. A. Drocco *et al.*, *Phys. Rev. Lett.* **95**, 088001 (2005).
- [8] L. E. Silbert, A. J. Liu, and S. R. Nagel, *Phys. Rev. Lett.* **95**, 098301 (2005); *Phys. Rev. E* **73**, 041304 (2006).
- [9] W. G. Ellenbroek *et al.*, *Phys. Rev. Lett.* **97**, 258001 (2006).
- [10] N. Xu and C. S. O’Hern, *Phys. Rev. E* **73**, 061303 (2006).
- [11] J. M. Schwarz, A. J. Liu, and L. Q. Chayes, *Europhys. Lett.* **73**, 560 (2006).
- [12] C. Toninelli, G. Biroli, and D. S. Fisher, *Phys. Rev. Lett.* **96**, 035702 (2006).
- [13] S. Henkes and B. Chakraborty, *Phys. Rev. Lett.* **95**, 198002 (2005).
- [14] M. Wyart, S. R. Nagel, and T. A. Witten, *Europhys. Lett.* **72**, 486 (2005); M. Wyart *et al.*, *Phys. Rev. E* **72**, 051306 (2005); C. Brito and M. Wyart, *Europhys. Lett.* **76**, 149 (2006).
- [15] V. Trappe *et al.*, *Nature (London)* **411**, 772 (2001).
- [16] T. S. Majmudar *et al.*, *Phys. Rev. Lett.* **98**, 058001 (2007).
- [17] A. S. Keys *et al.*, *Nature Phys.* **3**, 260 (2007).
- [18] M. Schröter *et al.*, *Europhys. Lett.* **78**, 44004 (2007).
- [19] R. Yamamoto and A. Onuki, *Phys. Rev. E* **58**, 3515 (1998).
- [20] L. Berthier and J.-L. Barat, *J. Chem. Phys.* **116**, 6228 (2002).
- [21] F. Varnik, L. Bocquet, and J.-L. Barrat, *J. Chem. Phys.* **120**, 2788 (2004).
- [22] D. J. Evans and G. P. Morriss, *Statistical Mechanics of Non-Equilibrium Liquids* (Academic, New York, 1990).
- [23] T. Hatano, M. Otsuki, and S. Sasa, *J. Phys. Soc. Jpn.* **76**, 023001 (2007).
- [24] In general, one should consider nonlinear scaling variables. In our case, the most important correction would be to replace  $\rho - \rho_c$  in Eq. (6) by  $g_\rho(\rho, \sigma) \equiv \rho - \rho_c + c\sigma^2$ ; this could lead to noticeable corrections to our scaling equation near  $\rho = \rho_c$ . However, since we find  $\Delta > 0.5$ , our conclusion that  $\eta^{-1} \sim \sigma^{\beta/\Delta}$  at  $\rho = \rho_c$  remains valid. See A. Aharony and M. E. Fisher, *Phys. Rev. B* **27**, 4394 (1983).
- [25] L. Berthier *et al.*, *Science* **310**, 1797 (2005).
- [26] A. Tanguy *et al.*, *Phys. Rev. B* **66**, 174205 (2002).